Published in final edited form as:
RSC Adv. 2015 January 8; 5(12): 8753–8756. doi:10.1039/C4RA16593D.

Alginate-peptide amphiphile core-shell microparticles as a targeted drug delivery system

Job Boekhoven[a,b], **R. Helen Zha**[a,e], **Faifan Tantakitti**[a,b], **Ellen Zhuang**[b], **Roya Zandi**[b], **Christina J. Newcomb**[a,f], and **Samuel I. Stupp**[a,b,c,d]

[a] Simpson Querrey Institute for BioNanotechnology, 303 E. Superior Ave, Chicago, IL 60611

[b] Department of Chemistry, Department of Biomedical Engineering and Department of Chemical Engineering, Northwestern University, Tech Building, 2145 Sheridan Road, Evanston, IL 60208

[c] Department of Materials Science and Engineering, Northwestern University, Cook Hall, 2220 Campus Drive, Evanston, IL 60208

[d] Department of Medicine, Feinberg School of Medicine, Galter Pavilion, 251 E. Huron St., Chicago, IL 60611

Abstract

We describe in this work the synthesis of microparticles with a doxorubicin drug conjugated alginate core and a shell of peptide amphiphile nanofibres functionalized for targeting the folate receptor. The spherical geometry of the particle core allows high drug loading per surface area, whereas the nanoscale fibrous shell formed by self-assembly of peptide amphiphiles offers a high surface to volume ratio that is ideal for targeting. The synthesised microparticles have a 60-fold higher cytotoxicity against MDA-MB-231 breast cancer cells compared to non-targeting particles.

Targeted drug delivery is a promising strategy to overcome the side effects of systemic drug-based therapies, including chemotherapy.[1] The targeting strategies investigated so far include the conjugation of monoclonal antibodies,[2] peptides,[3] aptamers[4] or small molecules[5] to drug carriers.[6] One of the small molecules investigated previously for targeting purposes is folate, a vitamin B analog that binds with high affinity to the membrane bound folate receptor overexpressed in many cancer cells.[7] We describe here the synthesis and *in vitro* testing of a microparticle containing an alginate drug-containing core and a fibrous nanoscale shell generated by self-assembly of peptide amphiphiles functionalized with folate.

Nanofibre-forming peptide amphiphiles (PAs) were first reported by Hartgerink et al.[8], and programming of their self-assembly into bioactive forms has evolved to make use of

Correspondence to: Samuel I. Stupp.

[e]Current address: Institute for Complex Molecular Systems, Eindhoven University of Technology, Den Dolech 2, 5612 AZ Eindhoven, Netherlands

[f]Current address: Physical Sciences Division, Pacific Northwest National Laboratory, Richland, WA 99352

† Electronic Supplementary Information (ESI) available: [details of any supplementary information available should be included here]. See DOI: 10.1039/b000000x/

molecules with 4 domains, (i) a hydrophobic tail, (ii) a peptide domain with a tunable β-sheet forming propensity,[9] (iii) a charged domain to increase solubility and (iv) a bioactive domain.[10] These PAs self-assemble in water driven by hydrophobic collapse of the tails and β-sheet formation of the second domain. The hydrogen bonds in the β-sheets provide directionality to the assemblies resulting in a fibrillar architecture. The fourth domain can be placed at the terminus away from the hydrophobic tail in order to display the bioactive cues at the surface of the fibre.[11] Such cues can be receptor binding peptide epitopes from extracellular proteins, enzyme substrates, or artificial peptides to bind specific proteins or serve as ligand mimics. Their functions might be differentiation of cells,[12] cell survival through biological adhesion,[13] angiogenesis,[14] proliferation of cells,[15] and amplification of growth factor signalling,[16] among others. PA nanofibres have also been investigated as drug carriers either through encapsulation in their hydrophobic core,[17] or covalent conjugation of the drug[18]. In this work, we have combined the high drug loading capacity of a polymeric microparticle with the high surface area of a nanoscale fibrous shell in which the PA's terminal domain is used to target drug delivery to cells overexpressing a specific receptor.

Previous work reported on the hierarchical assembly of cationic PA nano-fibres with anionic biopolymers to form macroscopic sacs in which the biopolymer is encapsulated within a fibrous PA-biopolymer hybrid membrane.[19] This concept has been miniaturised using a picospray strategy resulting in microcapsules having diameters 20-100 μm in diameter.[20] In this work, we have developed a new method to synthesize PA-coated microparticles with a tuneable diameter in the range of 600 nm to 2.3 μm.

The microparticles were synthesized by first forming an all-aqueous emulsion[21] by dispersing sodium alginate in sodium dextran sulphate (Fig. 1a and b). The addition of divalent calciumions to this emulsion selectively cross-links the alginate droplets. By means of dynamic light scattering (DLS) the size distribution of the particles was analysed and found to be tuneable by the amount of emulsified alginate in the range of roughly 600 nm to 2.3 μm (ESI). Next, the isolated particles were coated with a layer of cationic nanofibres formed by the self-assembly of C_{16}-$V_3A_3K_3$ by submerging the microparticles in a solution of PA. Fluorescence microscopy and scanning electron microscopy (SEM) (Fig. 1b and c) confirmed the successful coating of the microparticles with PA nanofibres. In order to use the coated particles as drug carriers, alginate was covalently modified with doxorubicin in a reversible manner, prior to particle formation. Alginate was first reacted with hydrazine, which converted 14% of the carboxylates to hydrazides, to afford compound **2** (Fig. 1e). The hydrazide **2** yielded hydrazone **3** upon reaction with doxorubicin. Hydrazones are dynamic labile bonds often used for sustained drug release,[22] and their hydrolysis is catalysed by acidic conditions.[23] We thus expected the release rate of doxorubicin to be higher in the acidic environments of the tumour cell.[24] Covalent attachment of doxorubicin to alginate did not affect the formation of alginate microparticles.

The release of doxorubicin from gels of **3** at pH 5, 6, or 7.4 was investigated by a colorimetric assay. At each pH, the maximum released amount of doxorubicin was reached after 110 h and, surprisingly, the release profile was similar for each pH value (ESI).

Also, the final relative amount of released doxorubicin reached a similar value for each pH of roughly 60%. We hypothesise that either the pH is locally affected by the presence of "buffering" alginate carboxylate groups or the diffusion of doxorubicin out of the alginate gel is the rate-determining step. A viability assay on MDAMB-231 breast cancer cells showed that the released doxorubicin was equally cytotoxic as commercial doxorubicin,[25] with half maximal inhibitory concentration (IC_{50}) values of 0.64 ± 0.2 μM for the released doxorubicin and 1.12 ± 0.4 μM for the commercial doxorubicin (ESI).

We grafted folate groups covalently to C_{16}-$V_3A_3K_3$ via a lysine linker (Fig. 2a) in order to target the doxorubicin-containing particles to cells overexpressing the folate receptor. Using the solvatochromic probe Nile Red,[26] the assemblies of C_{16}-$V_3A_3K_3$-NH_2 (**PA1**) and C_{16}-$V_3A_3K_4$-(*folate*)-NH_2 (**PA2**) were probed for the onset of hydrophobic collapse indicating their assembly (Fig. 2b). Both PAs assembled to form hydrophobic domains at a critical aggregation concentration (CAC) of roughly 10 μM. For **PA1**, a plateau at a blueshift of 18 nm was observed between 50 and 900 μM. At higher concentrations, the hydrophobicity increased further to level off at a blueshift of 30 nm, likely to be the result of a morphological transition. **PA2** reached a plateau of 27 nm blueshift and it should be noted that **PA2** appeared insoluble at a concentration above 500 μM. All further experiments were performed at a total PA concentration of 500 μM with 0, 10 or 20% **PA2** diluted in **PA1**.

In order to confirm that the morphology of the PA assemblies is similar with or without **PA2**, we characterized them by circular dichroism (CD, Fig. 2c) and cryogenic-transmission electron microscopy (Cryo-TEM, Fig. 2d). The CD spectra of all solutions revealed the presence of a ß-sheet secondary structure. Cryo-TEM of **PA1** solutions showed the presence of cylindrical fibres with diameters of roughly 10 nm, corresponding to twice the length of a fully extended PA. For solutions with up to 20% **PA2**, similar fibres were observed. Based on these observations, we conclude that incorporation of up to 20% **PA2** in diluent **PA1** does not affect the morphology of the supramolecular assemblies significantly.

In order to confirm the preferential uptake of PA fibres bearing a folate group, MDA-MB-231 breast cancer cells, known to overexpress the folate receptor, were incubated in solutions with 500 μM PA with 0, 10 or 20% **PA2** and 5% of rhodamine-bearing PA and either imaged or collected for flow cytometry analysis. Microscopy showed that the PA fibres, both with and without **PA2**, bind to MDA-MB-231 cells (ESI). The non-selective binding is most likely a result of ionic interactions between the highly cationic fibres and the negatively charged cell membrane. The binding of the PA mixtures was quantified by flow cytometry and confirmed that 100% of the cells had bound the cationic fibres as compared to a non-treated control (ESI). Interestingly, the fibres with 10% and 20% **PA2** showed a 1.6 and 1.4 fold higher mean fluorescence, respectively, as compared to fibres without **PA2**.

We investigated the uptake of fluorescent microparticles with a shell of **PA1** fibres containing 0%, 10% or 20% **PA2** by MDA-MB-231 cells. Fluorescence microscopy showed association of the particles with the cells for all ratios of **PA2**. However, the amount of cells with particles increased with **PA2** (Fig. 3a). Flow cytometry confirmed that 38% of the cells incubated in solution of particles with only **PA1** had particles associated to them (Fig. 3c). However, the fraction of cells that associated with particles increased to 72% and 59% in the

case of incubation with particles with 10 or 20% **PA2**, respectively. Our findings point to non-specific association of the particles and an increased uptake in the case of 10 or 20% **PA2**, presumably induced by folate receptor mediated endocytosis. We hypothesise that the cationic particles with and without **PA2** associate with the anionic membrane of the cells. Upon complexation the particles are in proximity of the folate receptor and the particles with **PA2** can be taken up via folate receptor mediated endocytosis. To confirm the non-specific interaction between cells and particles without **PA2** and the endocytotic uptake of particle with **PA2**, a confocal study was performed. Indeed, cells treated with particles without **PA2** showed association with particles on the cell membrane. On the other hand, cells treated with particles bearing **PA2** revealed both non-specific interactions between the cells and particles that appeared on the inside of the cell (Fig. 3b).

A viability assay showed that the particles without doxorubicin were not toxic towards MDA-MB-231 cells (ESI). Particles with doxorubicin did show toxicity and the particles without **PA2** had an IC50 value of 1.4 mM, expressed in concentration of doxorubicin. Interestingly, this value decreased nearly 60-fold to 24 μM doxorubicin for particles with 10% **PA2** and 20-fold to 70 μM for particles with 20% **PA2**. As a control, the same experiment was performed in the presence of free folate, which saturates the folate receptor and thereby prevents uptake of particles. Indeed, with 1 mM free folate, the particles show an IC50 value of 1.2 mM (ESI). The increased toxicity of **PA2** bearing particles confirms our hypothesis that cells only take up particles with **PA2**. These particles can subsequently release doxorubicin inside of the cell resulting in the observed increased toxicity. We speculate that the increased toxicity of particles with 10% **PA2** as compared to 20% **PA2** is a result of the molecular orientation of the folate groups on the supramolecular fibres, as has been observed for different bioactive cues.[13a, 27]

We have reported here on a new synthesis method of a soft core-shell microparticle consisting of a polymer core and a peptide amphiphile shell. Since the core is spherical it has a relatively high volume to surface area making it ideal for high loading densities, whereas the shell is made of high surface area to volume ratio fibres, ideal for targeting purposes. To demonstrate the potential of these particles as targeted drug delivery vehicles, we have conjugated the polymer core with doxorubicin and the fibres with a folate receptor targeting moiety. Particles with a targeting shell were found to be 60 times more toxic than their non-targeting counterparts against MBMDA-231 cancer cells. We believe that the combination of drug loaded polymer particles with high surface area peptide amphiphile fibres can provide a general platform for drug delivery vehicles.

Synthesis of the microparticles has been supported by the Non-Equilibrium Energy Research Center (NERC), an Energy Frontiers Research Center (EFRC) funded by the US Department of Energy, Office of Science, Office of Basic Energy Sciences under Award Number DE-SC0000989, and the authors are also grateful for support of the biological studies via a NIH-NIBIB Bioengineering Research Partnership grant (BRP, number 5R01EB003806-09). JB is grateful for support by a Netherlands Organisation for Scientific Research (NWO) Rubicon Fellowship. We would like to acknowledge the following core facilities at Northwestern University: EPIC Facilities of the NUANCE Center, Biological Imaging Facility, the Simpson Querrey Institute for BioNanotechnology.

Supplementary Material

Refer to Web version on PubMed Central for supplementary material.

References

1. a Rajendran L, Knölker HJ, Simons K. Nat. Rev. Drug. Discov. 2010; 9:29–42. [PubMed: 20043027] b Leamon CP, Reddy JA. Adv. Drug. Deliv. Rev. 2004; 56:1127–41. [PubMed: 15094211]
2. Wu Y, Cain-Hom C, Choy L, Hagenbeek TJ, de Leon GP, Chen Y, Finkle D, Venook R, Wu X, Ridgway J, Schahin-Reed D, Dow GJ, Shelton A, Stawicki S, Watts RJ, Zhang J, Choy R, Howard P, Kadyk L, Yan M, Zha J, Callahan CA, Hymowitz SG, Siebel CW. Nature. 2010; 464:1052–7. [PubMed: 20393564]
3. Sugahara KN, Teesalu T, Karmali PP, Kotamraju VR, Agemy L, Greenwald DR, Ruoslahti E. Science. 2010; 328:1031–5. [PubMed: 20378772]
4. McNamara JO, Andrechek ER, Wang Y, Viles KD, Rempel RE, Gilboa E, Sullenger BA, Giangrande PH. Nat. Biotechnol. 2006; 24:1005–15. [PubMed: 16823371]
5. Weissleder R, Kelly K, Sun EY, Shtatland T, Josephson L. Nat. Biotechnol. 2005; 23:1418–23. [PubMed: 16244656]
6. a Branco MC, Schneider JP. Acta. Biomater. 2009; 5:817–31. [PubMed: 19010748] b Rösler A, Vandermeulen GW, Klok H-A. Adv. Drug. Delivery Rev. 2012; 64:270–279.
7. Salazar MD, Ratnam M. Cancer Metastasis Rev. 2007; 26:141–52. [PubMed: 17333345]
8. Hartgerink JD, Beniash E, Stupp SI. Science. 2001; 294:1684–8. [PubMed: 11721046]
9. Newcomb CJ, Sur S, Ortony JH, Lee OS, Matson JB, Boekhoven J, Yu JM, Schatz GC, Stupp SI. Nat. Commun. 2014; 5:3321. [PubMed: 24531236]
10. Guler MO, Hsu L, Soukasene S, Harrington DA, Hulvat JF, Stupp SI. Biomacromolecules. 2006; 7:1855–1863. [PubMed: 16768407]
11. Boekhoven J, Stupp SI. Advanced. Materials. 2014; 26:1642–1659. [PubMed: 24496667]
12. Silva GA, Czeisler C, Niece KL, Beniash E, Harrington DA, Kessler JA, Stupp SI. Science. 2004; 303:1352–5. [PubMed: 14739465]
13. a Storrie H, Guler MO, Abu-Amara SN, Volberg T, Rao M, Geiger B, Stupp SI. Biomaterials. 2007; 28:4608–18. [PubMed: 17662383] b Khan S, Sur S, Dankers PY, da Silva RM, Boekhoven J, Poor TA, Stupp SI. Bioconjugate. Chem. 2014; 25:707–717.
14. a Rajangam K, Arnold MS, Rocco MA, Stupp SI. Biomaterials. 2008; 29:3298–305. [PubMed: 18468676] b Chow LW, Bitton R, Webber MJ, Carvajal D, Shull KR, Sharma AK, Stupp SI. Biomaterials. 2011; 32:1574–82. [PubMed: 21093042]
15. Webber MJ, Tongers J, Newcomb CJ, Marquardt KT, Bauersachs J, Losordo DW, Stupp SI. Proc. Natl. Acad. Sci. U.S.A. 2012; 109:9220.
16. Lee SS, Huang BJ, Kaltz SR, Sur S, Newcomb CJ, Stock SR, Shah RN, Stupp SI. Biomaterials. 2013; 34:452–459. [PubMed: 23099062]
17. Soukasene S, Toft DJ, Moyer TJ, Lu H, Lee HK, Standley SM, Cryns VL, Stupp SI. ACS. Nano. 2011; 5:9113–21. [PubMed: 22044255]
18. Matson JB, Stupp SI. Chem. Commun. 2011; 47:7962–4.
19. Capito RM, Azevedo HS, Velichko YS, Mata A, Stupp SI. Science. 2008; 319:1812–6. [PubMed: 18369143]
20. Rożkiewicz DI, Myers BD, Stupp SI. Angew. Chem. Int. Ed. 2011; 123:6448–6451.
21. Walter, H.; Brooks, DE.; Fisher, D., editors. Aqueous Two – Phase System: Theory, Methods, Uses, And applications to Biotechnology. Academic press; London: 1985. Partitioning.
22. Matson JB, Stupp SI. Chem. Commun. 2011; 47:7962–4.
23. a Janeliunas D, van Rijn P, Boekhoven J, Minkenberg CB, van Esch JH, Eelkema R. Angew. Chem. Int. Ed. Engl. 2013; 52:1998–2001. [PubMed: 23319333] b Boekhoven J, Poolman JM, Maity C, Li F, van der Mee L, Minkenberg CB, Mendes E, van Esch JH, Eelkema R. Nature. Chem. 2013; 5:433–437. [PubMed: 23609096]

24. Tannock IF, Rotin D. Cancer Res. 1989; 49:4373–4384. [PubMed: 2545340]

25. Tegze B, Szállási Z, Haltrich I, Pénzváltó Z, Tóth Z, Likó I, Gyorffy B. PLoS. One. 2012; 7:e30804. [PubMed: 22319589]

26. a Boekhoven J, Brizard AM, van Rijn P, Stuart MC, Eelkema R, van Esch JH. Angew. Chem. Int. Ed. Engl. 2011; 50:12285–12289. [PubMed: 21761526] b Boekhoven J, Rubert Pérez CM, Sur S, Worthy A, Stupp SI. Angew. Chem. Int. Ed. Engl. 2013; 52:12077–12080. [PubMed: 24108659]

27. Webber MJ, Tongers J, Renault MA, Roncalli JG, Losordo DW, Stupp SI. Acta Biomater. 2010; 6:3–11. [PubMed: 19635599]

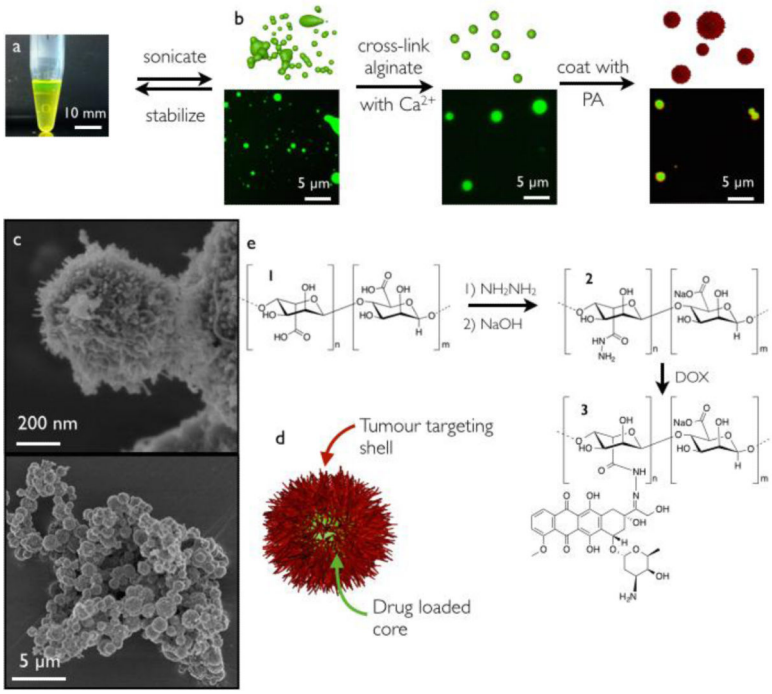

Fig. 1.

a) Photograph of an aqueous-two-phase system of dextran-sulphate (bottom) and fluorescein conjugated alginate (top). b) Schematic representation of microparticle synthesis (top) supported by fluorescence microscopy micrographs (bottom). Alginate is labelled with fluorescein (green) and the PA is labelled with rhodamine (red). c) SEM micrographs of dried microparticles coated with a PA layer. d) Schematic representation of the final microparticle. e) Synthesis of alginate derivatives **1, 2** and **3**.

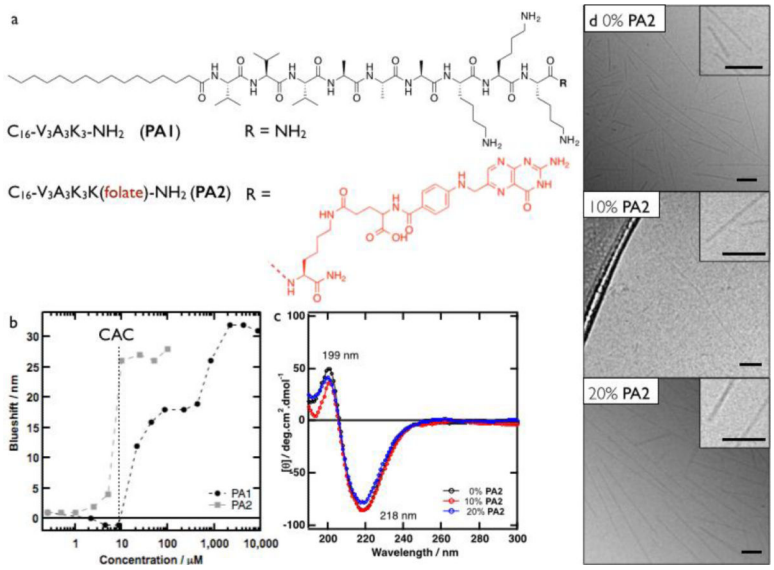

Fig. 2.

a) Structures of **PA1** and **PA2**. b) Nile Red blue shift as a function PA concentration c) CD spectra of 500 μM PA at varying ratios of **PA1**:**PA2** (0, 10 and 20% **PA2**). d) Cryo-TEM micrographs of 500 μM PA at varying ratios of **PA1**:**PA2** (0, 10 and 20% **PA2**). All scale bars are 100 nm.

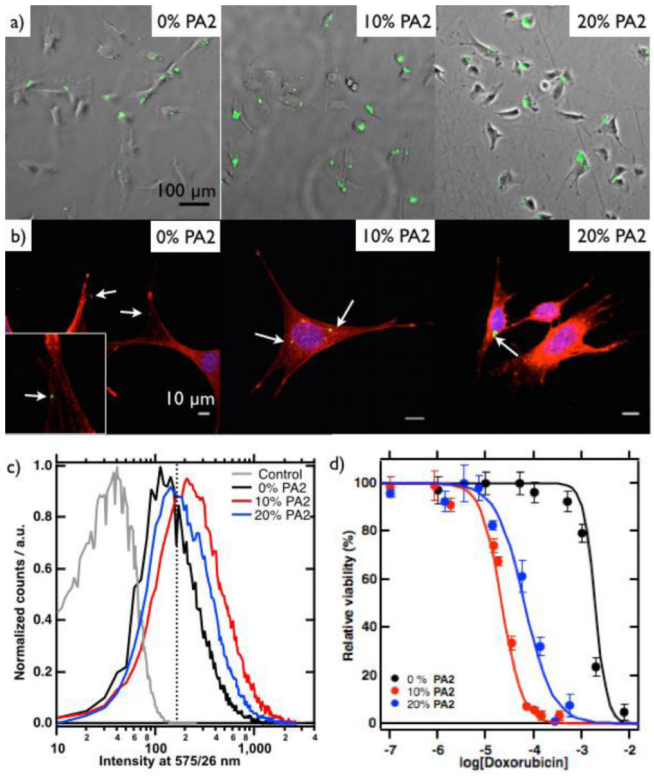

Fig. 3.

a) Fluorescence microscopy images over brightfield microscopy images of MDA-MB-231 cells incubated with particles (green) with nanofibres with varying ratios of **PA1** and **PA2**. b) Confocal microscopy images of MDA-MB-231 cells (actin filaments red, nuclei blue) incubated with particles (green). c) Histogram of flow cytometry data from MDA-MB-231 cells incubated with varying ratios of **PA2** and 5% rhodamine-PA. Samples were excited at 561 nm. d) Relative viability against concentration of particles, expressed as concentration of doxorubicin.